

# We are IntechOpen, the world's leading publisher of Open Access books Built by scientists, for scientists

6,900

Open access books available

186,000

International authors and editors

200M

Downloads

Our authors are among the

154

Countries delivered to

TOP 1%

most cited scientists

12.2%

Contributors from top 500 universities



WEB OF SCIENCE™

Selection of our books indexed in the Book Citation Index  
in Web of Science™ Core Collection (BKCI)

Interested in publishing with us?  
Contact [book.department@intechopen.com](mailto:book.department@intechopen.com)

Numbers displayed above are based on latest data collected.  
For more information visit [www.intechopen.com](http://www.intechopen.com)



# Tunable Dielectric Microwave Devices with Electromechanical Control

Yuriy Poplavlo, Yuriy Prokopenko and Vitaliy Molchanov  
National Technical University of Ukraine "Kiev Polytechnic Institute"  
Ukraine

## 1. Introduction

One of the trends of modern telecommunication systems development is use of high-tunable passive components, such as tunable resonators, phase shifters, etc. These components are the key elements of smart antennas, phased-array antennas, tunable oscillators, filters and so on. Many ways are known to design tunable microwave system:

- $\mu(H)$ : tuning of ferrite material permeability by magnetic field;
- $\varepsilon(E)$ : tuning of ferroelectric material permittivity by electric field;
- $\sigma(E)$ : tuning of semiconductor material conductivity by electric field;
- $\sigma(\Phi)$ : optical impact tuning of semiconductor material conductivity under light beam  $\Phi$ ;
- $\Delta$ : tuning by the mechanical reconfiguration of resonant (or transmission) part of microwave subsystem.

Components with magnetic and electric tuning, such as  $\mu(H)$ ,  $\sigma(E)$  (Campbell & Brown, 2000; Ellinger et al., 2001; Lucyszyn & Robertson, 1992) and also  $\varepsilon(E)$  (Rao et al., 1999; Deleniv et al., 2003; Kim et al., 2005) have frequency limitation of about 30-40 GHz due to the increased loss at higher frequencies. Optical tuning that exploits conductivity change  $\sigma(\Phi)$  (Lee et al., 1999; Ling et al., 2005) under the light beam  $\Phi$  also introduces considerable loss at the millimeter waves. Therefore, usual tunable components that control material's intrinsic properties  $\mu(H)$ ,  $\sigma(E)$ , or  $\varepsilon(E)$  have fundamental limitations at millimeter waves. The main reason is that microwaves interact with "active" material (ferrite, semiconductor, or ferroelectric) which is a part of microwave line, and transmitted energy is partially absorbed in this material.

On the contrary, the mechanical system of control is not a part of microwave propagation route so it does not contribute to the microwave loss. One but important disadvantage of mechanical control is a relatively low tuning speed.

Recent achievements in the piezoelectric actuator and MEMS technologies open an opportunity to combine advantages of mechanical and electrical tuning techniques. However, for such applications the tuning system should be highly sensitive to rather small displacement of device's components. The key question is how to achieve such high sensitivity of the system characteristics to small displacement of device's parts. This could be achieved if parts displacement provides strong perturbation of the electromagnetic field distribution. For that a variable dielectric discontinuity (the air gap) is created on the way of

the electric field lines. This air gap is placed between the dielectric parts or the dielectric and an electrode. An alteration of the air gap dimension leads to substantial transformation in electromagnetic field distribution and changes such components characteristics as resonant frequency, phase of propagating wave and so on.

This transformation could be described in terms of medium's effective dielectric permittivity ( $\epsilon_{eff}$ ). Effective dielectric permittivity of inhomogeneous medium is dielectric permittivity, which brings numerically same macro parameters to the system of the same geometrical configuration. Effective permittivity is convenient parameter to describe devices with TEM wave propagating, where propagation constant is proportional to  $\sqrt{\epsilon_{eff}}$ . But it can be used to describe other devices as well. For example, effective permittivity of partially loaded waveguide can be stated as such permittivity of fully loaded waveguide, which gives numerically the same propagation constant as in partially loaded waveguide.

## 2. Tunable effective dielectric constant

The simplest example of a tunable effective dielectric constant is a waveguide partially filled with dielectric, Fig. 1. The air gap between dielectric material and broad wall of waveguide dramatically reduces measured value of dielectric permittivity, and it is the main component of measurement uncertainty. This fact is well known for waveguide technique of dielectric permittivity measurement. However, this phenomenon is applicable for tunable devices design as well (Jeong et al, 2002).

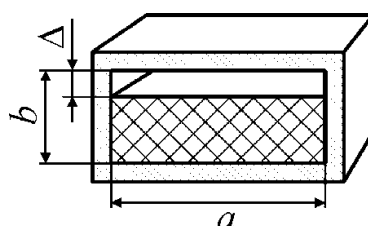


Fig. 1. Partially filled waveguide

Effective permittivity for the basic mode of rectangular waveguide can be found as:

$$\epsilon_{eff} = \frac{\left(\frac{\pi}{a}\right)^2 + \gamma^2}{k^2},$$

where  $\gamma$  is the propagation constant,  $k$  is the wave number in free space, and  $a$  is the width of waveguide.

The results of effective permittivity simulation are presented in Fig. 2. As one can see, there is a strong influence of air gap onto effective parameters, especially for high- $\epsilon$  materials. The main reason of such high sensitivity is the location of dielectric discontinuity. The air gap is located across electrical field of waveguide's basic mode and acts as strong perturbation of electromagnetic field, which value depends on air gap's size  $\Delta$ .

One of possible uses of effective permittivity transformation is tuning of phase shifters. The nature of the phase shift can be explained with Fig. 3. Wavelength in dielectric filled part of

waveguide is shortened proportionally to  $\sqrt{\epsilon_{eff}}$ . Because of partial loading of waveguide, there is the nonzero component  $E_z$  of electric field in the direction of propagation. In combination with the component  $E_y$ , which is orthogonal to media boundary, it gives resultant vector  $E$ , which crosses media boundary at certain slope. Refraction at the dielectric media boundary changes slope of resultant vector  $E$ . So, traveling wave makes its path of two ways: one inside of dielectric, and another one in the air. Because of refraction, the ratio of the way in dielectric and air respectively changes as air gap changes. Simply speaking, the control over the traveling wave phase shift is obtained by the varying part of the way, which wave travels outside of dielectric.

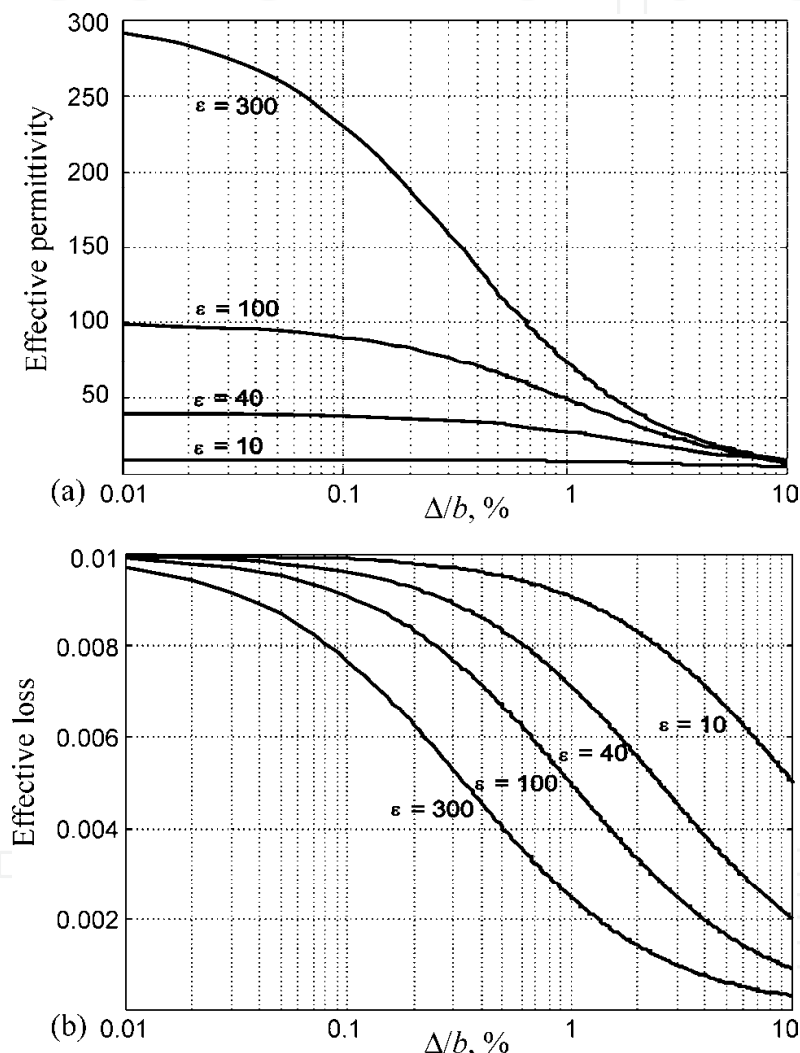


Fig. 2. Effective parameters of partially loaded waveguide: a) effective permittivity; b) effective loss;  $\Delta$  is the air gap,  $b$  is the waveguide height

This idea was verified experimentally (Jeong et al., 2002). Phase shifter was made inside of rectangular waveguide section. It can be made either in symmetric or asymmetric fashion (the last is shown in Fig. 4). Controlled element consists of dielectric slab supported by the metal plate. This plate is rigidly attached to the piezoelectric actuator. Under applied control

voltage the air gap  $\Delta$  is controlled via actuators variable extension. Parameters of used dielectric materials are listed in Table I.

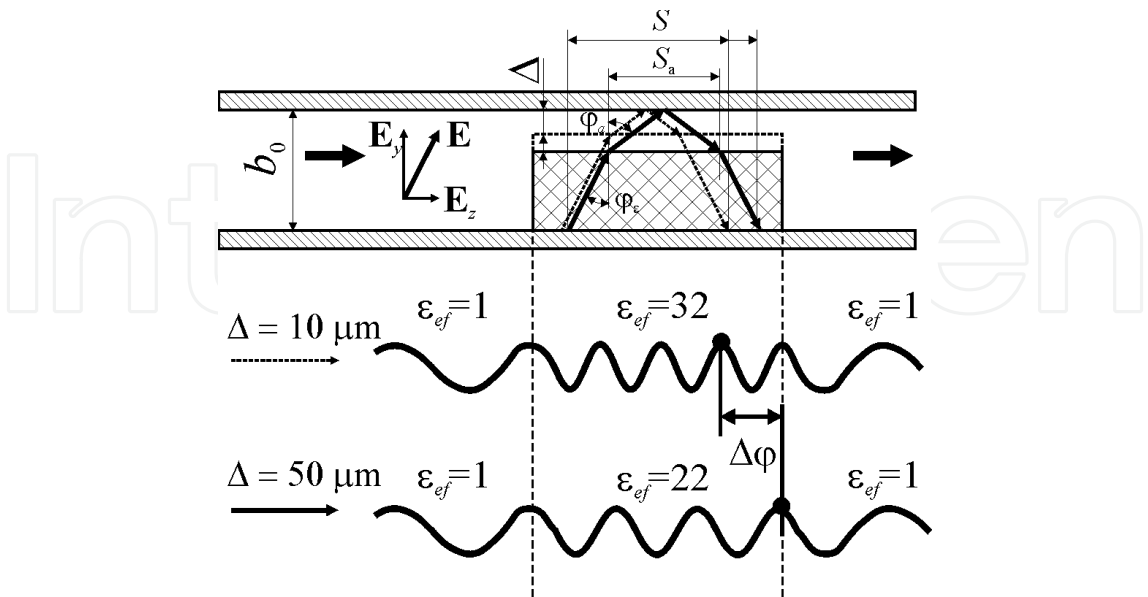


Fig. 3. Phase shift nature in partially loaded waveguide

Material	$\epsilon$	$\tan\delta$ @ 10 GHz	$\tan\delta$ @ 40 GHz
$\text{Al}_2\text{O}_3$	11.6	$0.7 \cdot 10^{-4}$	$4 \cdot 10^{-4}$
$(\text{Mg,Ca})\text{TiO}_3$	21	$2 \cdot 10^{-4}$	$8 \cdot 10^{-4}$
$\text{BaTi}_4\text{O}_9$	37	$3 \cdot 10^{-4}$	$10^{-3}$
BLT	85	$2 \cdot 10^{-3}$	—

Table I. Parameters of used dielectric materials

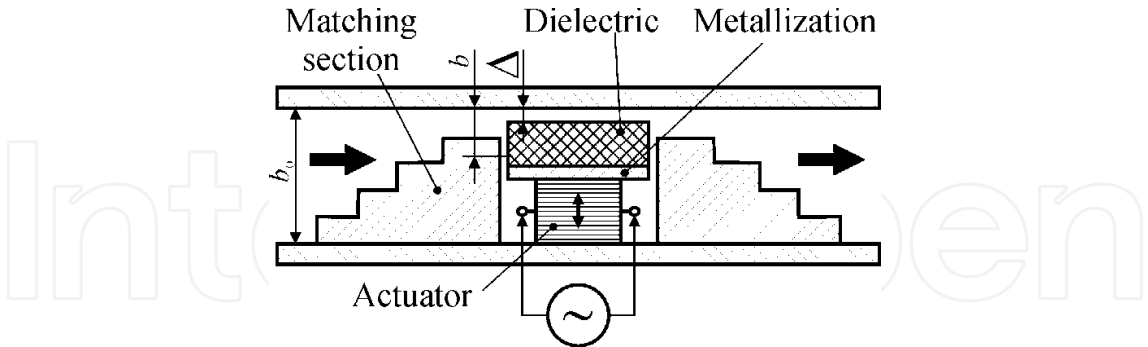


Fig. 4. Waveguide phase shifter experimentally studied design

Fig. 5 illustrates measured control curves. They have almost linear character and promising values. Fig. 6 demonstrates measured  $S$ -parameters of the phase shifter. It is expected that increase of operation frequency can make this design competitive with solid state devices.

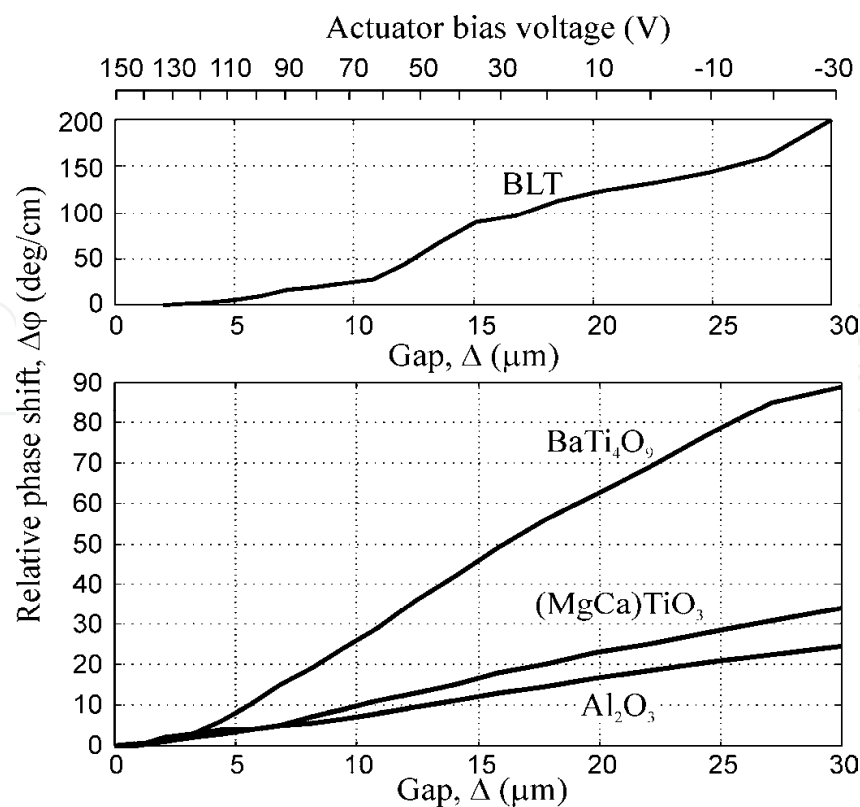


Fig. 5. Measured control curves @10.5 GHz

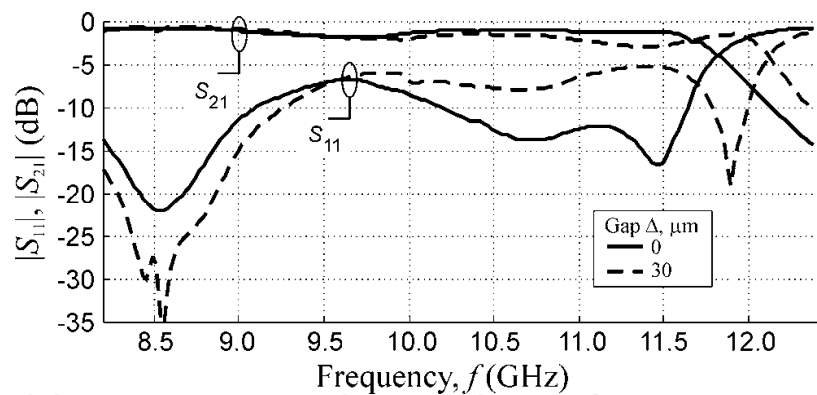


Fig. 6. Measured S-parameters of the device. Dielectric plate of 1mm height and 10 mm length made of material with  $\epsilon = 21$

### 3. Tunable dielectric resonators

Electromechanical control of high quality dielectric resonator frequency is known for a long time. One of the examples is two cylindrical dielectric resonators with the  $H_{01\delta}$  mode separated by the air slot ( $\Delta$ ), constituting a binary dielectric resonator, Fig. 7, a (Wakino et al., 1987). Electric field components in the binary dielectric resonator are located in its basic plane. In contrast, a split dielectric resonator (Poplavko et al., 2001), also of  $H_{01\delta}$  type, has a slot located athwart to the electric field components for the lowest resonant mode (Fig. 7, b). This split dielectric resonator shows much larger tunability than binary dielectric resonator, as it is shown in Fig. 7, c.

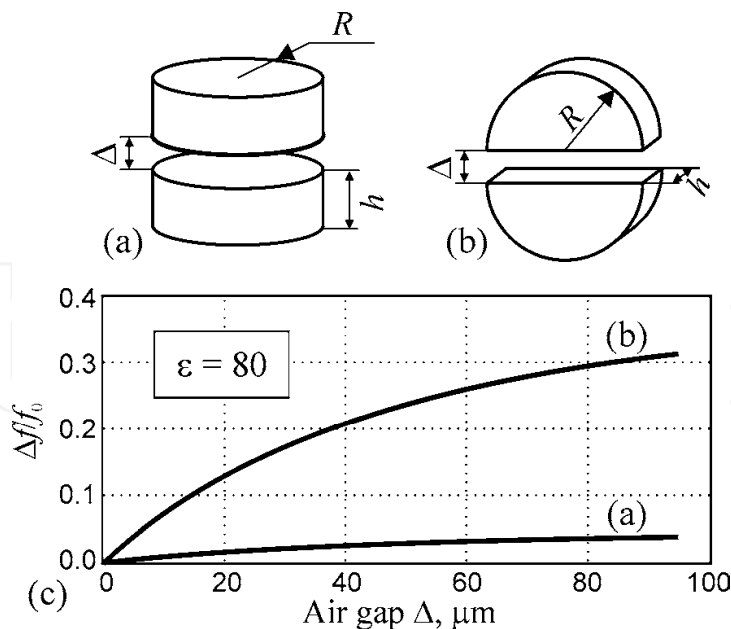


Fig. 7. dielectric resonator mechanical tuning at 10 GHz: (a) ordinary manner; (b) proposed manner; (c) characteristics comparison

One example of split dielectric resonator testing is shown in Fig. 8. No change in a quality factor  $Q$  is observed during air slot alteration. Conformable split dielectric resonators are used in the high- $Q$  tunable filter (about 20%) in a waveguide near the central frequency of 10 GHz (Poplavko et al., 2001).

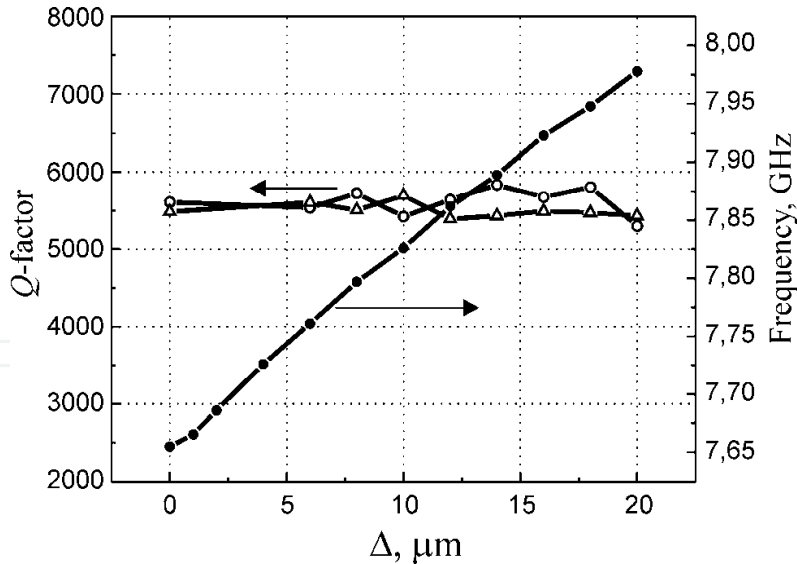


Fig. 8. Resonant frequency  $f_0$  and  $Q$ -factor of split dielectric resonator vs. slot

Tunability of the split dielectric resonator can be explained as the alteration in the split dielectric resonator’s effective permittivity ( $\epsilon_{eff}$ ), Fig. 9.

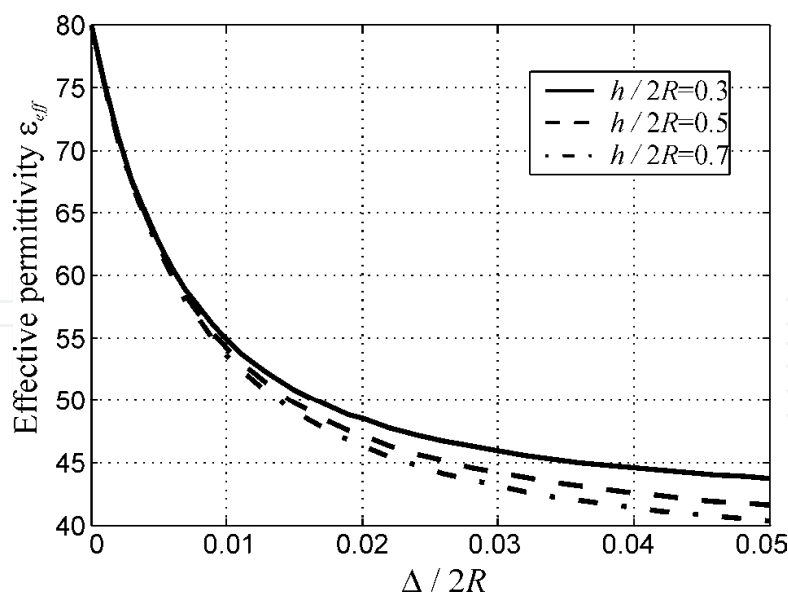


Fig. 9. Effective permittivity versus normalized value of air gap between two parts of disk dielectric resonator shown in Fig. 1b. Permittivity of dielectric material is equal to 80;  $D$  is dielectric resonator diameter while  $h$  is dielectric resonator thickness.

In the considered case, the value of  $\epsilon_{eff}$  decreases about 2 times; correspondingly, split dielectric resonator resonant frequency increases up to 30%. Tunability slightly rises with the ratio of  $h / 2R$  where  $R$  is split dielectric resonator radius, and  $h$  is its thickness. An advantage of such method of frequency control is high  $Q$ -factor preservation. The unloaded quality factor can be expressed as  $Q_0^{-1} = T \tan \delta$ , where  $T$  is the energy filling factor, which depends only on dielectric constant and domain size ( $\tan \delta$  is the loss tangent of dielectric material). Due to electromagnetic energy accumulation in a slot the factor  $T$  shows a trend to decrease, Fig. 10. As a result, intrinsic  $Q$ -factor of the split dielectric resonator can even rise with resonant frequency increase.

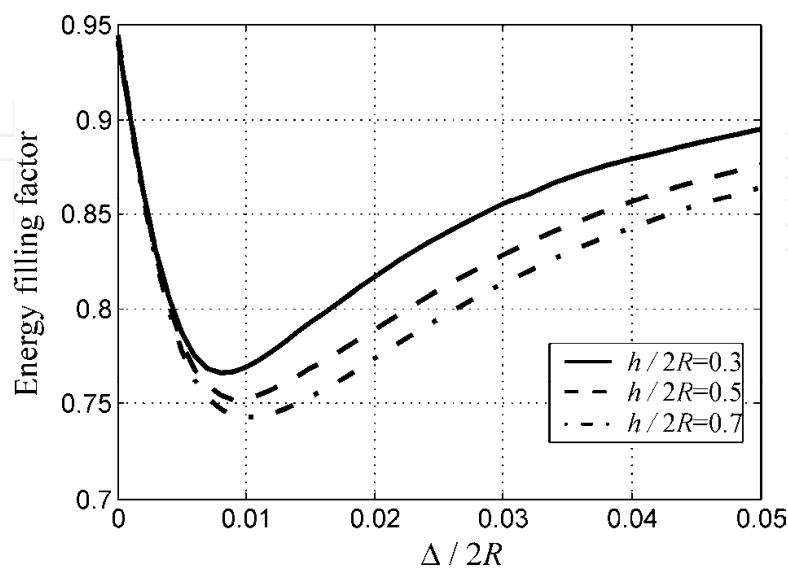


Fig. 10. Energy filling factor versus normalized value of air gap between two parts of cylindrical dielectric resonator. Dielectric constant of material is 80



This frequency control method could be applied to split dielectric resonator of different shapes, including rectangular, ring or sphere. Rectangular and spherical split dielectric resonator are shown in Fig. 11, and their effective permittivity dependences are shown in Fig. 12.

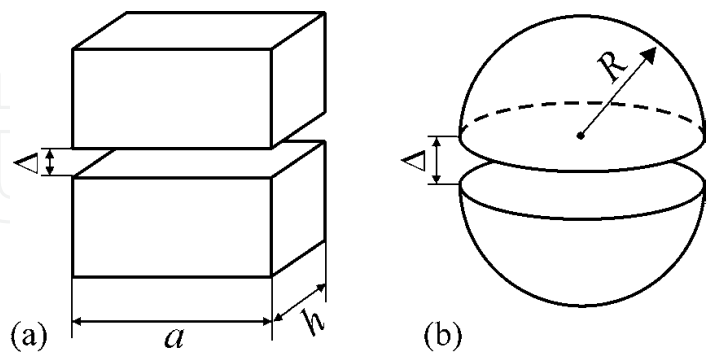


Fig. 11. Rectangular and spherical split dielectric resonator

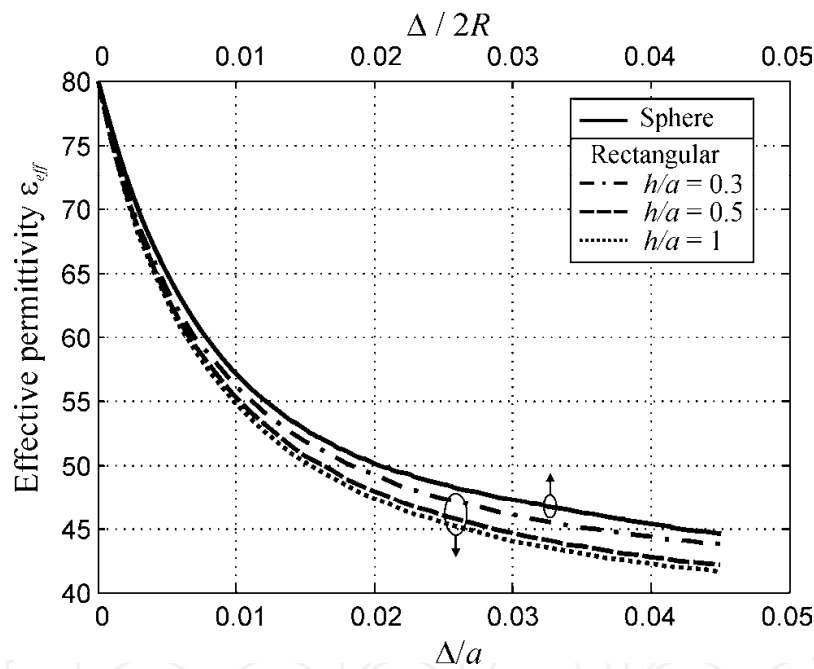


Fig. 12. Effective permittivity of rectangular and spherical split dielectric resonators

4. Electromechanically tunable microstrip phase shifter

Principal designs of piezo-driven phase shifter based on the microstrip line are shown in Fig. 13. Experiments and calculations show that their phase shift is strongly dependent on design architecture. Only one of designs (shown in Fig. 13, a) was published previously (Yun & Chang, 2002).

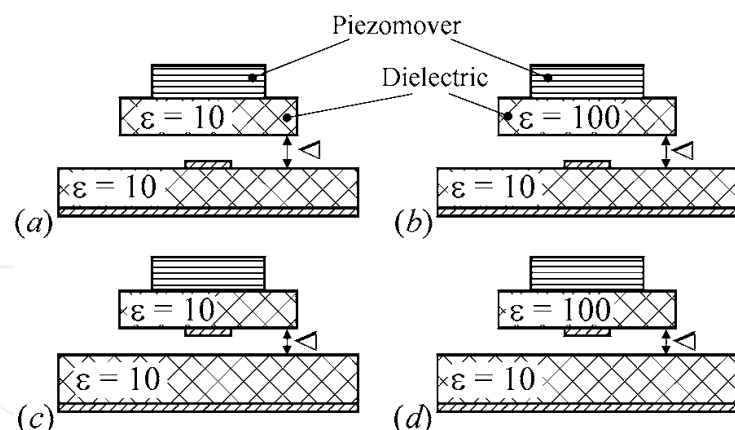


Fig. 13. Mechanically tuned microstrip phase shifters.

However, it is obvious that other designs shown in Fig. 13, b, c, d shows higher effect because dielectric discontinuity is created in the plane perpendicular to electrical field of the microstrip line. The effectiveness was verified and proved experimentally. The best result is obtained with the new idea of “detached” upper electrode, Fig. 13, c, d that is electrode disconnected from substrate and attached to the moveable dielectric plate. Close to these cases phase shift would be obtained if the bottom electrode would be disconnected. Simulation in Fig. 14 confirms that stronger perturbation of electromagnetic field distribution results in higher differential phase shift.

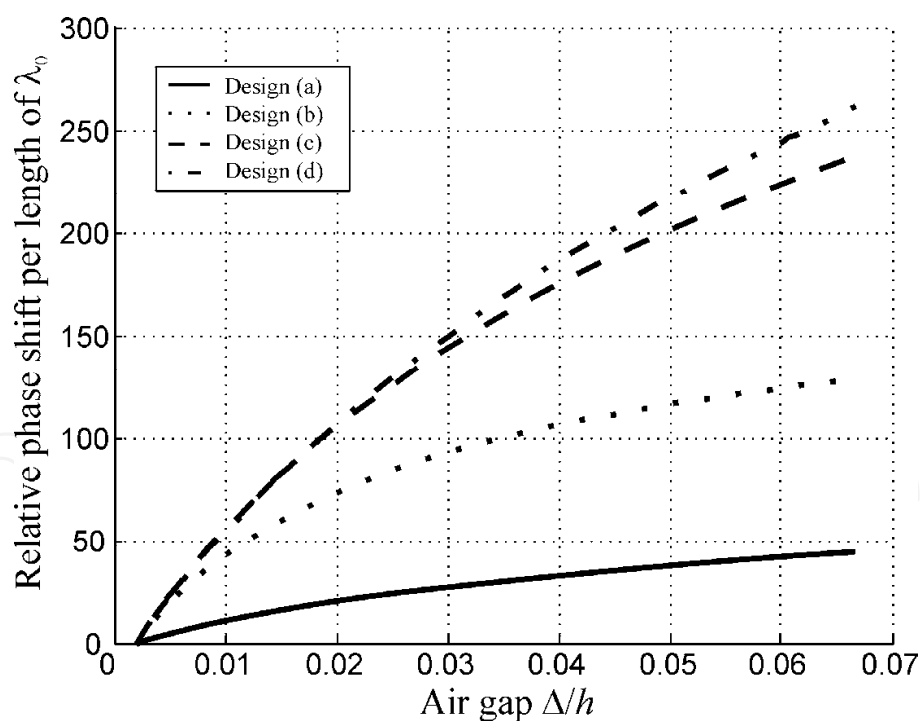


Fig. 14. Comparison of known (a) and new proposed devices (b, c, d). Phase shift (standardized on wavelength) is shown as function of tunable air gap

This effect also could be explained in terms of effective permittivity change. As one can see in Fig. 15, designs with detachable electrode exhibit larger change in effective dielectric constant, which in turn is observed as larger phase shift.

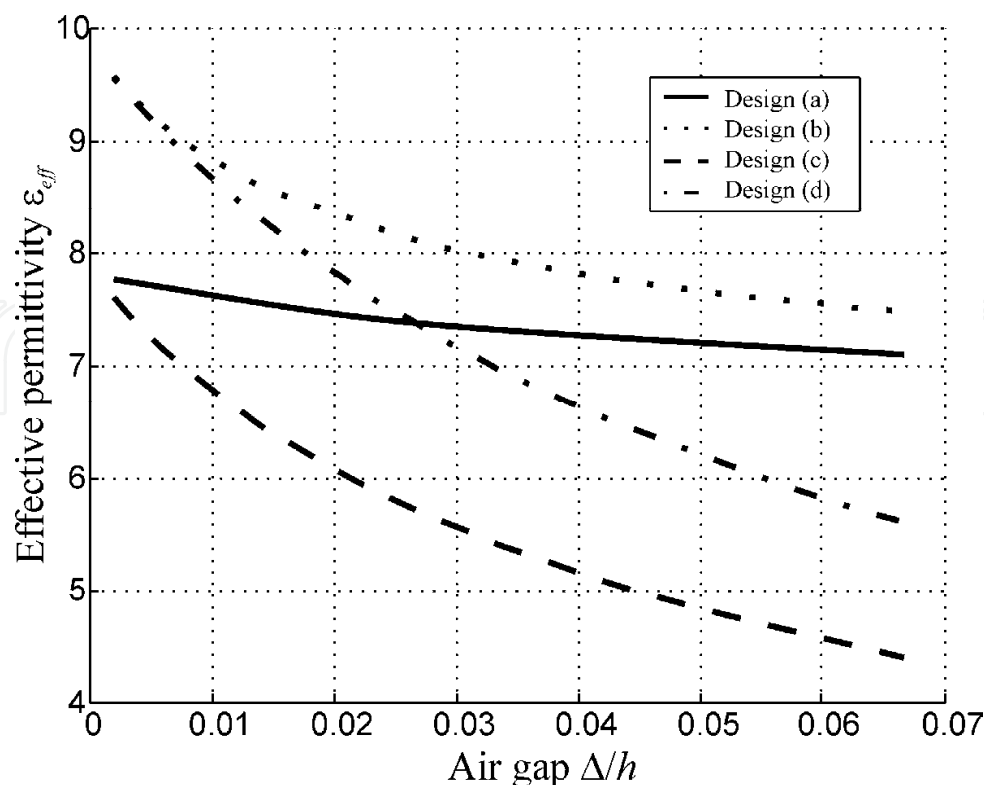


Fig. 15. Comparison of effective dielectric permittivity  $\epsilon_{eff}$  in known (a) and new proposed devices (b, c, d)

In other words, propagation constant at a given frequency  $f$  can be estimated as  $\gamma = \frac{2\pi f}{c} \sqrt{\epsilon_{eff}}$  where  $c$  is the light velocity. So the main task of device analysis is to determine effective permittivity for prescribed geometrical configuration. This problem is solved numerically using finite element method.

5. Two resonators impedance-step filter controlled from bottom

Principal design and characteristics of a band-transmitting filter (that can be used as a phase shifter) is shown in Fig. 16 together with filter’s characteristics. Experimental result was obtained with the network analyzer. Filter is arranged on the right-angled alumina substrate where two impedance steps resonators are deposited (the length of resonator is 22 mm, the ratio between high and low impedance parts ~10, substrate thickness 0,65 mm, substrate dielectric constant  $\epsilon = 9,2$ ).

With the purpose of tuning, the substrate, located under the filter, imitates a “tunable dielectric”. Namely, the part of ground electrode (just under the coupling part of filter) is removed and substituted by the piezoelectric actuator, which is closely adjacent to the substrate, Fig. 17.

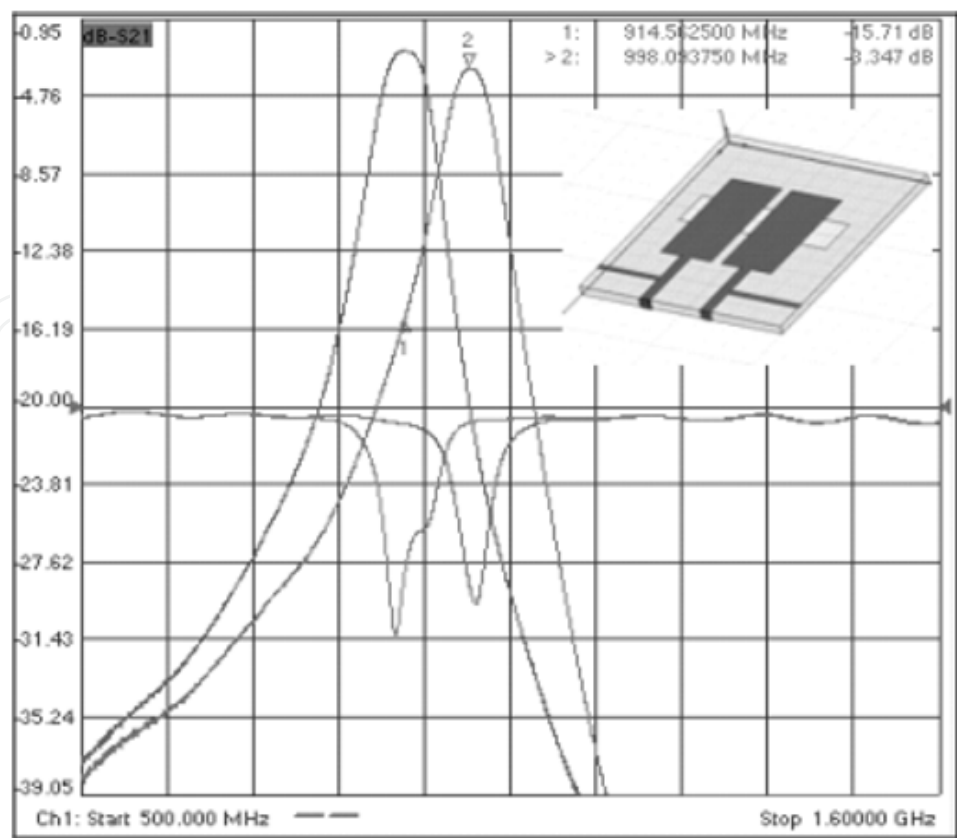


Fig. 16. Two-resonator tunable filter design and characterization.

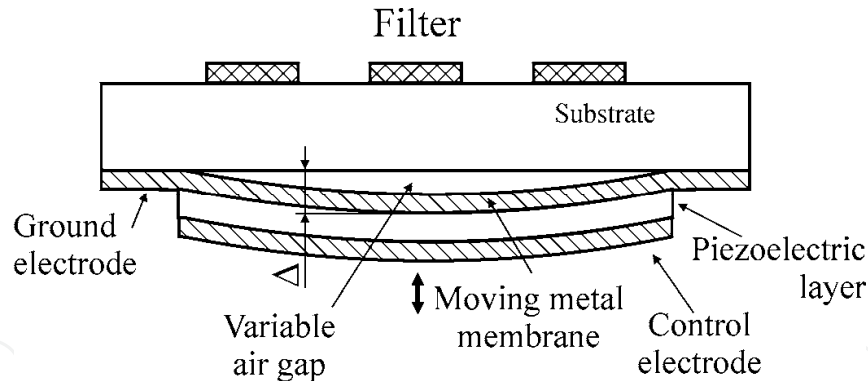


Fig. 17. The concept of filter tuning: side view of moving ground electrode under the substrate.

Actuator’s upper electrode is simultaneously a ground electrode of the substrate. Due to the actuator, the thickness of the narrow air gap ( $\Delta$ ) is electrically controlled. Such a “tunable substrate” can be described as dielectric in which effective permittivity is controlled. The scope of the  $\epsilon_{eff}$  change depends on the substrate  $\epsilon$  and relationship  $\Delta/h$  where  $h$  is substrate thickness. In our experiments the effective permittivity of the layered dielectric “alumina – air” decreases from  $\epsilon_{eff} \approx 7$  till  $\epsilon_{eff} \approx 3$  while the range of a gap change was from  $\Delta \sim 10\mu\text{m}$  till  $\Delta \sim 100\mu\text{m}$  under the voltage of about 300 V.

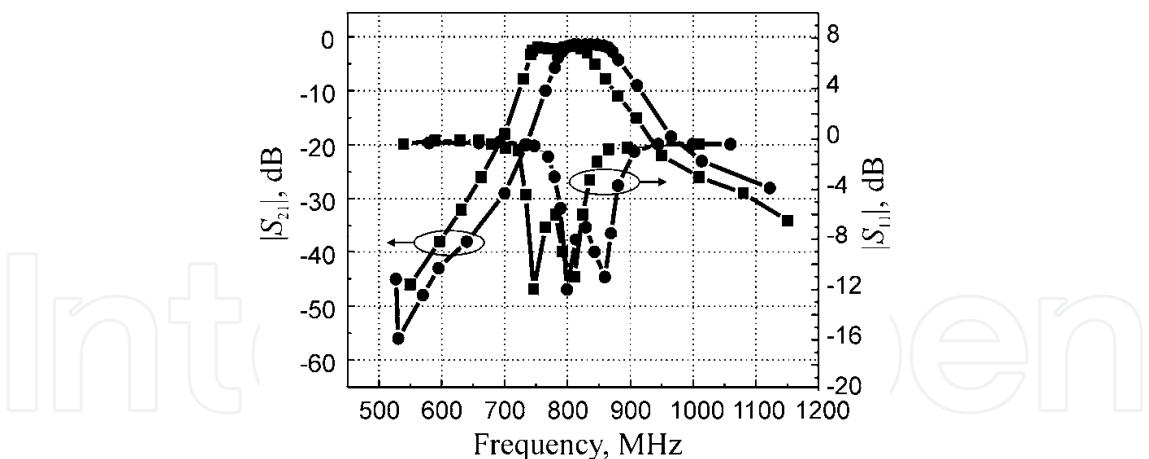


Fig. 18. Filter characteristics for two positions of dielectric plate: central resonant frequency shifts of about 10% while filter attenuation remains less than 1 dB.

Calculation and tuning of studied structures was made by the method of the FEM simulation. The results of calculation show good agreement with the experiment. Any tunable band-pass filter can be used as a phase shifter but only at the frequency range of its bandwidth. In a given experiment this bandwidth looks rather narrow, and controlling voltage seems too big for many applications. That is why another design and different way of filter controlling is proposed below. Experimental prototype of studied “*tunable filter – phase shifter*” is shown on photograph.

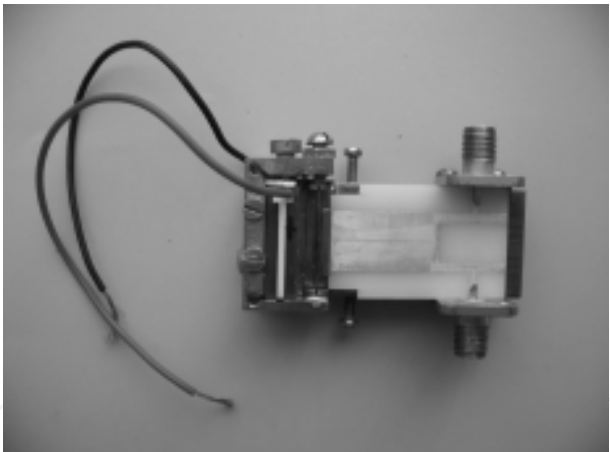


Fig. 19. Photo of experimental prototype.

6. Electromechanically tunable coplanar line

Electromagnetic field of microwave transmission lines deposited onto substrate is mainly confined in the substrate right under electrodes and in the inter-electrode space to certain degree. Because of that the dielectric body is moved up and down above the line’s surface, as it is shown in Fig. 20, a, makes small perturbation of electromagnetic field distribution. To improve device’s controllability it is necessary to arrange tighter dependence of electromagnetic field on moving dielectric body position. For that it is proposed to situate a

signal strip of coplanar waveguide on moving dielectric body and let them lift together (Prokopenko et al., 2007), Fig. 20, b.

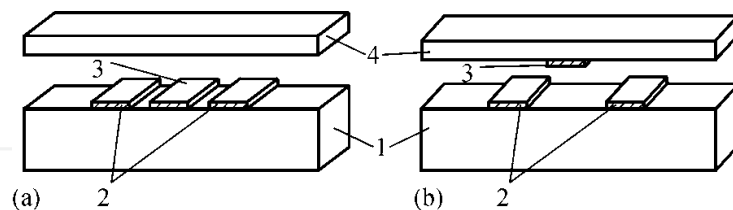


Fig. 20. Coplanar line based phase shifters with signal line: a – on the substrate, b – on the moving dielectric body. 1 – substrate, 2 – ground electrodes, 3 – signal line, 4 – moving dielectric body

Fig. 21 shows simulations of near  $50\ \Omega$  coplanar lines with dielectric permittivity of both substrate and movable dielectric body  $\epsilon=12$  for presented in Fig. 20 designs. Here and after relative phase shift is calculated for the device of length equal to wavelength in vacuum. Qualitative conclusion is that under other same conditions the device with detaching electrode exhibits greater relative effective permittivity change, and thus its relative phase shift more than 1.5 times exceeds one from counterpart.

Obviously, strong perturbation of electromagnetic field improves device's controllability. But quantitatively it depends on a number of design factors, such as line geometry, impedance and ratio of the substrate's and movable dielectric permittivity. Generally low impedance lines tend to exhibit higher controllability. This can be achieved not only by use of high-permittivity materials, but with proper layout as well.

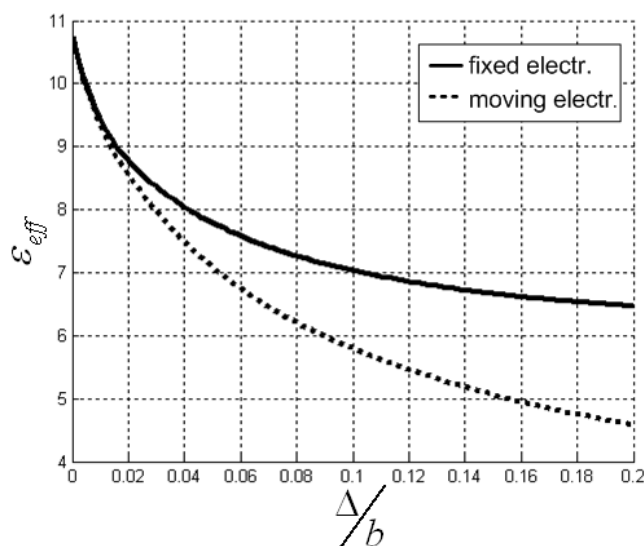


Fig. 21. Dependencies of effective permittivity of the coplanar line based phase shifters

To prove presented ideas, one scaled up experiment was performed. Experimental setup consists of coplanar dielectric ( $\epsilon = 4.3$ ) substrate in the aluminium fixture. The signal line is soldered to the bonding pads at the sides of the substrate (Fig. 22, a), whereas being glued to the moveable dielectric, which in turn is attached to micrometer screw (see the photo in Fig. 22, b).

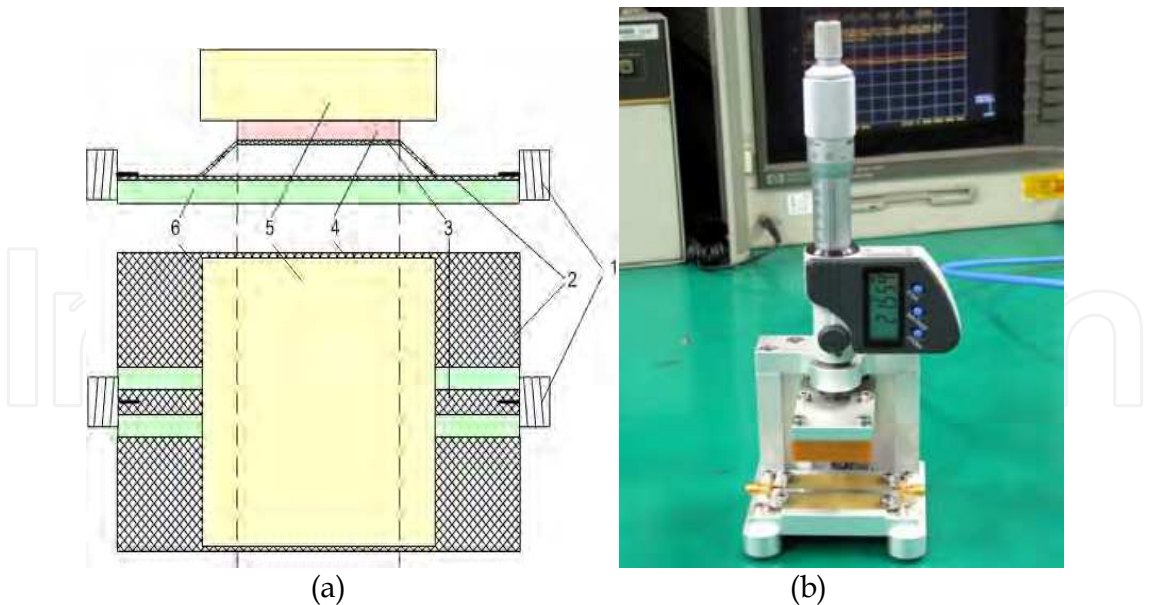


Fig. 22. Experimental setup: (a) – schematic, (b) – photo. 1 – connector; 2 – ground electrodes; 3 – movable electrode; 4 – movable dielectric; 5 – low-ε support; 6 – substrate

Fig. 23 and Fig. 24 present results of experimental investigation of the proposed phase shifters.

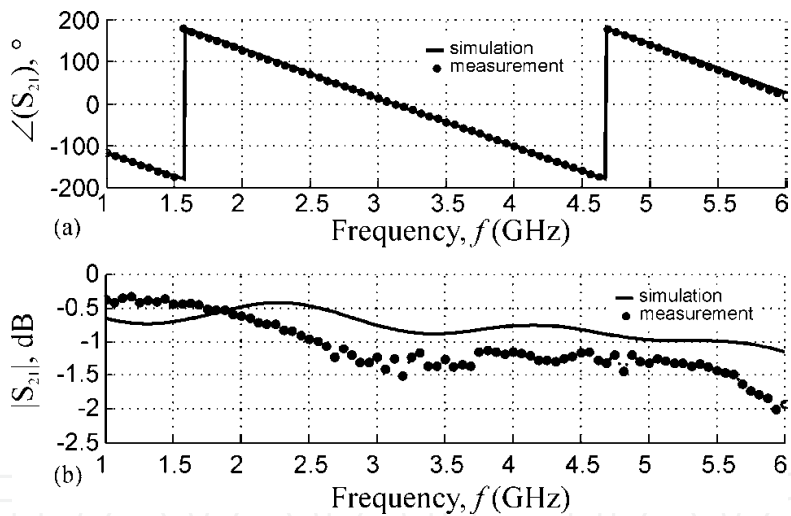


Fig. 23. Simulation and measurement of phase (a) and magnitude (b) of transmission coefficient  $S_{21}$  for the coplanar line based phase shifter with moving signal electrode

Fig. 25 presents simulation and measurement of control curve for both discussed designs. There is a good agreement between simulation and measurement result.

### 7. Conclusion

Main mechanisms of piezoelectric control by the  $\epsilon_{eff}$  of some devices based on dielectric layers are discussed. It is supposed that the most effective way is to use a composition “microwave dielectric – air gap”, controlled by the fast actuator. At that, a minimal loss is inserted in tunable component.



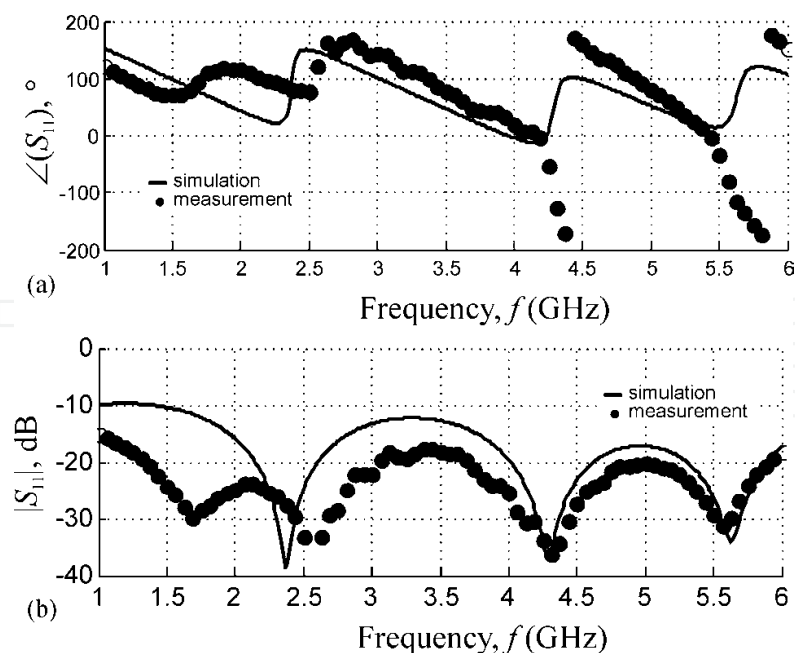


Fig. 24. Simulation and measurement of phase (a) and magnitude (b) of reflection coefficient  $S_{11}$  for the coplanar line based phase shifter with moving signal electrode

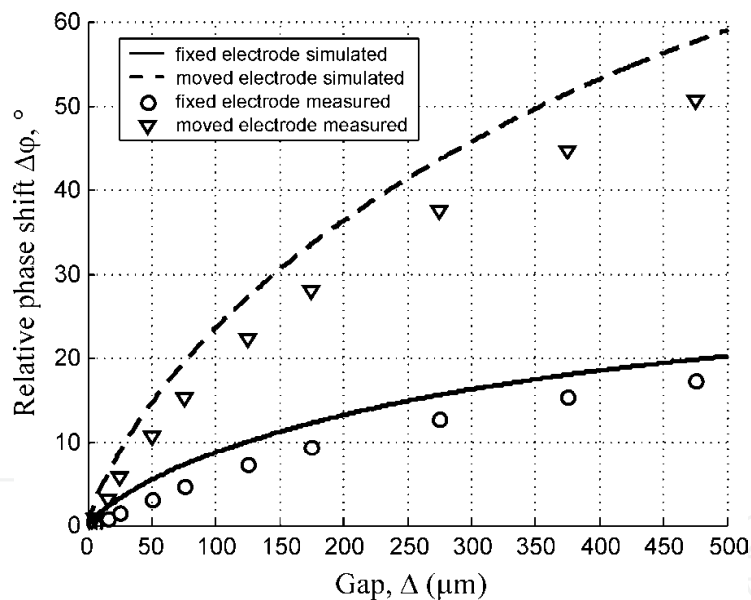


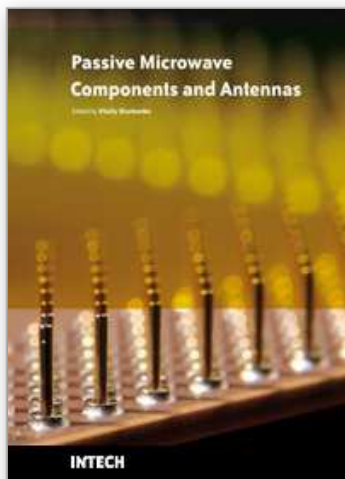
Fig. 25. Coplanar line controlled with teflon slab.  $f = 5$  GHz, Substrate:  $40 \times 30 \times 1.6$  mm,  $\epsilon = 4.3$ , Movable dielectric:  $30 \times 20 \times 1$  mm,  $\epsilon = 2.08$  Signal line width is 3 mm

Using high quality microwave dielectrics, it is possible to realize low loss filters and phase shifters as in the microwaves so as in the millimeter waves. Proposed structures are studied as in the rectangular waveguide, so in some microstrip designs. Proposed way of control allows to increase device’s controllability while maintain low loss. Simulations are proved by the experiment. With scaling down and move to the higher frequencies, the amount of required displacements could be reduced to tens micrometers, thus allowing an application of small size and fast piezo-actuators or MEMS.



## 8. References

- Campbell, C.F. & Brown, S.A. (2000). A compact 5-bit phase-shifter MMIC for K-band satellite communication systems. *IEEE Trans. Microwave Theory Tech.*, Vol. 48, (Dec. 2000), P. 2652–2656.
- Deleniv, A.; Abadei, S. & Gevorgian, S. (2003). Tunable ferroelectric filter-phase shifter. *IEEE MTT-S International Microwave Symposium Digest.*– June 2003.– Vol. 2, P. 1267–1270.
- Ellinger, F.; Vogt, R. & Bachtold, W. (2001). Compact reflective-type phase-shifter MMIC for C-band using a lumped-element coupler. *IEEE Trans. Microwave Theory Tech.*, Vol. 49, (May 2001), P. 913–917.
- Jeong, M.; Kazmirenko, V.; Poplavko, Y.; Kim, B. & Baik, S. (2002). Electrically Tunable Phase Shifters With Air-Dielectric Sandwich Structure. *Proceedings of Material Research Society Symp.*, pp. H3.12.1–H3.12.6, Vol. 720.
- Kim, Ki-Byoung; Yun, Tae-Soon; Kim, Hyun-Suk; Kim, Il-Doo; Kim, Ho-Gi & Lee, Jong-Chul. (2005). Coplanar ferroelectric phase shifter on silicon substrate with TiO<sub>2</sub> buffer layer. *Proceedings of European Microwave Conference*, pp. 649–652, ISBN 2-9600551-0-1, Paris France, Sep. 2005.
- Lee, S.-S.; Udupa, A. H.; Erlig, H.; Zhang, H.; Chang, Y.; Chang, D.H.; Bhattacharya, D.; Tsap, B.; Steier, W.H.; Dalton, L.R. & Fetterman, H.R. (1999). Demonstration of a photonicallly controlled RF phase shifter. *IEEE Microwave Guided Wave Lett.*, Vol. 9, (Sept. 1999), P. 357–359.
- Ling, Liao; Ansheng, Liu; Jones, R.; Rubin, D.; Samara-Rubio, D.; Cohen, O.; Salib, M. & Paniccia, M. (2005). Phase modulation efficiency and transmission loss of silicon optical phase shifters. *IEEE Journal of Quantum Electronics*, Vol. 41, (Feb. 2005), P. 250–257.
- Lucyszyn, S. & Robertson, I. D. (1992). Synthesis techniques for high performance octave bandwidth 180° analog phase shifters. *IEEE Trans. Microwave Theory Tech.*, Vol. 40, (Apr. 1992), P. 731–740.
- Poplavko, Yu.M.; Prokopenko, Yu.V.; Molchanov, V.I. & Dogan, A. (2001). Frequency-tunable microwave dielectric resonator. *IEEE Trans. Microwave Theory Tech.*, Vol. 49, (June 2001), P. 1020 – 1026.
- Poplavko, Y. ; Golubeva, I.; Kazmirenko, V.; Jeong, M. & Baik, S. (2005). Piezo-controlled Dielectric Phase Shifter with Microstrip and Coplanar Lines. *Proceedings of European Microwave Conference*, pp. 1335 – 1338, ISBN 2-9600551-0-1, Paris France, Sep. 2005.
- Prokopenko, Y.; Golubeva, I.; Kazmirenko, V. & Poplavko, Y. (2007). Coplanar line based low loss microwave phase shifters with electromechanical control. *Proceedings of European Microwave Conference*, pp. 1582–1585, Munich Germany, Oct. 2007.
- Rao, J.B.L.; Patel, D.P. & Krichevsky, V. (1999). Voltage-controlled ferroelectric lens phased arrays. *IEEE Trans. Antennas Propagat.*, Vol. 47, (Mar. 1999), P. 458–468.
- Wakino, K.; Tamura, H. & Ishikawa, Y. (1987). Dielectric resonator device, *USA Patent #4,692,727*, Sep.8, 1987.
- Yun, T.-Y. & Chang, K. (2002). Analysis and optimization of a phase shifter controlled by a piezoelectric transducer. *IEEE Trans. Microwave Theory Tech.*, Vol. 50, (January 2002), P. 105–111.



## **Passive Microwave Components and Antennas**

Edited by Vitaliy Zhurbenko

ISBN 978-953-307-083-4

Hard cover, 556 pages

**Publisher** InTech

**Published online** 01, April, 2010

**Published in print edition** April, 2010

Modelling and computations in electromagnetics is a quite fast-growing research area. The recent interest in this field is caused by the increased demand for designing complex microwave components, modeling electromagnetic materials, and rapid increase in computational power for calculation of complex electromagnetic problems. The first part of this book is devoted to the advances in the analysis techniques such as method of moments, finite-difference time-domain method, boundary perturbation theory, Fourier analysis, mode-matching method, and analysis based on circuit theory. These techniques are considered with regard to several challenging technological applications such as those related to electrically large devices, scattering in layered structures, photonic crystals, and artificial materials. The second part of the book deals with waveguides, transmission lines and transitions. This includes microstrip lines (MSL), slot waveguides, substrate integrated waveguides (SIW), vertical transmission lines in multilayer media as well as MSL to SIW and MSL to slot line transitions.

### **How to reference**

In order to correctly reference this scholarly work, feel free to copy and paste the following:

Yuriy Poplavlo, Yuriy Prokopenko and Vitaliy Molchanov (2010). Tunable Dielectric Microwave Devices with Electromechanical Control, *Passive Microwave Components and Antennas*, Vitaliy Zhurbenko (Ed.), ISBN: 978-953-307-083-4, InTech, Available from: <http://www.intechopen.com/books/passive-microwave-components-and-antennas/tunable-dielectric-microwave-devices-with-electromechanical-control>

**INTECH**  
open science | open minds

### **InTech Europe**

University Campus STeP Ri  
Slavka Krautzeka 83/A  
51000 Rijeka, Croatia  
Phone: +385 (51) 770 447  
Fax: +385 (51) 686 166  
[www.intechopen.com](http://www.intechopen.com)

### **InTech China**

Unit 405, Office Block, Hotel Equatorial Shanghai  
No.65, Yan An Road (West), Shanghai, 200040, China  
中国上海市延安西路65号上海国际贵都大饭店办公楼405单元  
Phone: +86-21-62489820  
Fax: +86-21-62489821

© 2010 The Author(s). Licensee IntechOpen. This chapter is distributed under the terms of the [Creative Commons Attribution-NonCommercial-ShareAlike-3.0 License](https://creativecommons.org/licenses/by-nc-sa/3.0/), which permits use, distribution and reproduction for non-commercial purposes, provided the original is properly cited and derivative works building on this content are distributed under the same license.

IntechOpen

IntechOpen